IEEE Access
Multidisciplinary | Rapid Review | Open Access Journal

Date of publication xxxx 00, 0000, date of current version xxxx 00, 0000.

Digital Object Identifier 10.1109/ACCESS.2017.Doi Number

PMU-based FOPID Controller of Large-scale Wind-PV Farms for LFO Damping in Smart Grid

Mahdi Saadatmand[1], Gevork B. Gharehpetian[2], (Senior Member, IEEE), Pierluigi Siano[3], (Senior Member, IEEE), Hassan Haes Alhelou[4], (Senior Member, IEEE)

[1] Power System Secure Operation Research Center, Amirkabir University of Technology, Tehran, Iran
[2] Department of Electrical Engineering, Amirkabir University of Technology, Tehran, Iran
[3] Department of Management & Innovation Systems, University of Salerno, 84084 Fisciano, Italy
[4] School of Electrical and Electronic Engineering, University College Dublin, Dublin 4, D04 V1W8, Ireland

Corresponding author: Hassan Haes Alhelou (e-mail: alhelou@ieee.org).

ABSTRACT Due to global warming problems and increasing environmental pollution, there is a strong tendency to install and apply renewable energy power plants (REPPs) around the world. On the other hand, with the increasing development of information and communication technology (ICT) infrastructures, power systems are using these infrastructures to act as smart grids. In fact, future modern power systems should be considered as smart grids with many small and large scale REPPs. One of the main problems and challenges of the REPPs is uncertainty and fluctuation of electrical power generation. Accordingly, a suitable solution can be combination of different types of REPPs. So, the penetration rate of large-scale wind-PV farms (LWPF) is expected to increase sharply in the coming years. Given that the LWPFs are added to the grid or will replace fossil fuel power plants, they should be able to play the important roles of synchronous generators such as power low-frequency oscillation (LFO) damping. In this paper, an LFO damping system is suggested for a LWPF, based on a phasor measurement unit (PMU)-based fractional-order proportional–integral–derivative (FOPID) controller with wide range of stability area and proper robustness to many power system uncertainties. Finally, the performance of the proposed method is evaluated under different operating conditions in a benchmark smart system.

INDEX TERMS Fractional-order proportional–integral–derivative (FOPID) controller, Low-Frequency Oscillation (LFO), Large-scale wind-PV Farm (LWPF), Power Oscillation Damping Controller (PODC), Phasor measurement unit (PMU), Smart Grid.

I. INTRODUCTION

Global warming, environmental pollutions and other destructive effects of fossil fuels-based power generation have led to a growing focus on the use of renewable energies around the world [1]. So, a growing trend can be seen in establishing and exploiting renewable energy power plants (REPPs) [2, 3]. This type of power plants is usually integrated with the main grid to increase generation capacity with low pollution. Moreover, they may replace conventional power plants in some cases [4, 5]. In other words, in future systems, the REPPs will play an important role in electrical power generation.

On the other hand, information and communication technology (ICT) infrastructures are rapidly developing, and also with the help of artificial intelligence (AI) systems, power systems can be considered as smart grids [6, 7]. A smart grid includes three layers. A power system layer, a control system layer and a communication infrastructure layer [6]. In transmission level, smart grids are based on wide-area measurement systems (WAMSs) that receive most of their desired data through the phasor measurement units (PMUs) [6]. The application of PMUs can reduce many uncertainties of REPPs, considering their accurate measurements, which can be used for any control system.

Despite the various benefits of renewable energy resources, some of the inherent characteristics of this type of energy resources are considered as challenges in their efficient use and are obstacles to proper efficiency and reliability in electricity generation [5]. For example, non-everlasting winds at the proper speed and the lack of solar irradiation at whole times are some of the challenges which can reduce the generation efficiency in the large-scale

This article has been accepted for publication in a future issue of this journal, but has not been fully edited. Content may change prior to final publication. Citation information: DOI 10.1109/ACCESS.2021.3094170, IEEE Access

photovoltaic farms (LPFs) and large-scale wind farms (LWFs). This causes high uncertainty in the power generation by these types of power plants [5]. Large-scale hybrid wind-PV farm (LWPF) is regarded as a fundamental solution for these challenges [8, 9]. These types of REPPs include two generator units, wind turbine generators (WTGs) and photovoltaic (PV) generators (PVGs). The hybrid application of WTGs and PVGs increases the efficiency and reliability of electrical power generation than the separated application of LPFs and LWFs [8, 9].

In order to exploit REPPs, two important issues need to be addressed. The operation of these power plants causes many changes in the characteristics of power systems such as stability. Given that REPPs are inverter-based, so they reduce mechanical inertia and can increase the risk of LFOs in the power system [10–13]. Moreover, given the replacement of REPPs with the conventional power plants, many of the existing capabilities in the synchronous generators, such as low-frequency oscillation (LFO) damping by power system stabilizer (PSS) should be performed by them. Therefore, the REPP needs to be able to mitigate the LFOs by a supplementary controller.

In many papers, the LFO damping through the LPFs and LWFs has been studied [14–20]. Given that the control model of the LWPF is different from the control model of conventional REPPs, it is necessary to investigate this issue separately, which has been investigated in [21], and a simple lead-lag controller (LLC) has been suggested as a power oscillation damping controller (PODC).

Although the LLC is very cheap and very common, it provides a smaller stability area than modern controllers and also has low robustness against grid uncertainties. One of the types of modern controllers that have been studied recently is the fractional-order proportional-integral-derivative (FOPID) controller, which is the general structure of proportional-integral-derivative (PID) controllers [22]. The FOPID controller is mathematically based on the fractional-order calculus [22-30]. Due to the inherent characteristics of the FOPID controllers, these types of controllers have a wide stability region. In addition, it is highly robust against power system uncertainties. In recent years, the application of this type of controller in the case of automatic generation control (AGC) [31], load-frequency control (LFC) [32], and LFOs damping by synchronous generators [33], FACTS devices [34], and LPFs [35, 36], has been the subject of many researches.

In this paper, the implementation of the PMU-based FOPID controller in the control loop of the LWPF for LFOs damping is proposed. For this purpose, an optimized tuning method based on teaching–learning-based optimization (TLBO) is proposed to obtain the values of the FOPID controller parameters. Finally, the performance of the controller is evaluated in various operating conditions and against different uncertainties in a smart grid.

The rest of the paper is organized as follows. Section 2 provides an overview of the LWPF, its benefits, and models for power system studies. The introduction of the FOPID controller and the concept of fractional-order calculus are given in Section 3. Also, the use of the FOPID controller as a PODC is proposed in section 4. Moreover, tuning of the proposed PODC, simulation, and performance evaluation are presented and discussed in Section 5. The conclusions are drawn in Section 6.

II. Overview of LWPF

The LWPFs are the new type of REPPs which are extensively used in the near future considering their higher efficiency and reliability, compared to the conventional REPPs [8, 9]. The hybrid application of WTGs and PVGs reduces the uncertainty of power generation [8, 9]. As shown in Figure 1, when PV generation decreases, the WTG may compensate for the shortage of the PV generation, and vice versa [37].

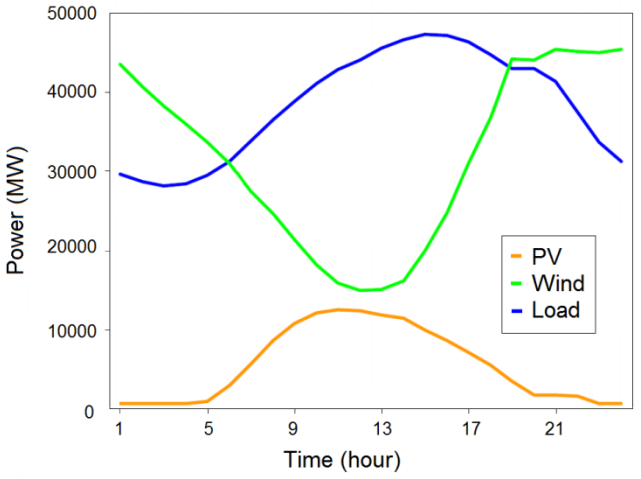

FIGURE 1. Average PV generation, wind generation, and load demand. California, USA, July 2003 [37].

Note that various types of small-scale hybrid generation systems are currently in operation. The LWPFs consist of four basic components including PVGs, WTGs, inverters, and controllers [1]. This type of power plants includes a separate controller for each generator and a central controller for the whole power plant. Each controller receives command signals from the central controller [38, 39]. Figure 2 illustrates the schematic structure of the LWPF.

This article has been accepted for publication in a future issue of this journal, but has not been fully edited. Content may change prior to final publication. Citation information: DOI 10.1109/ACCESS.2021.3094170, IEEE Access

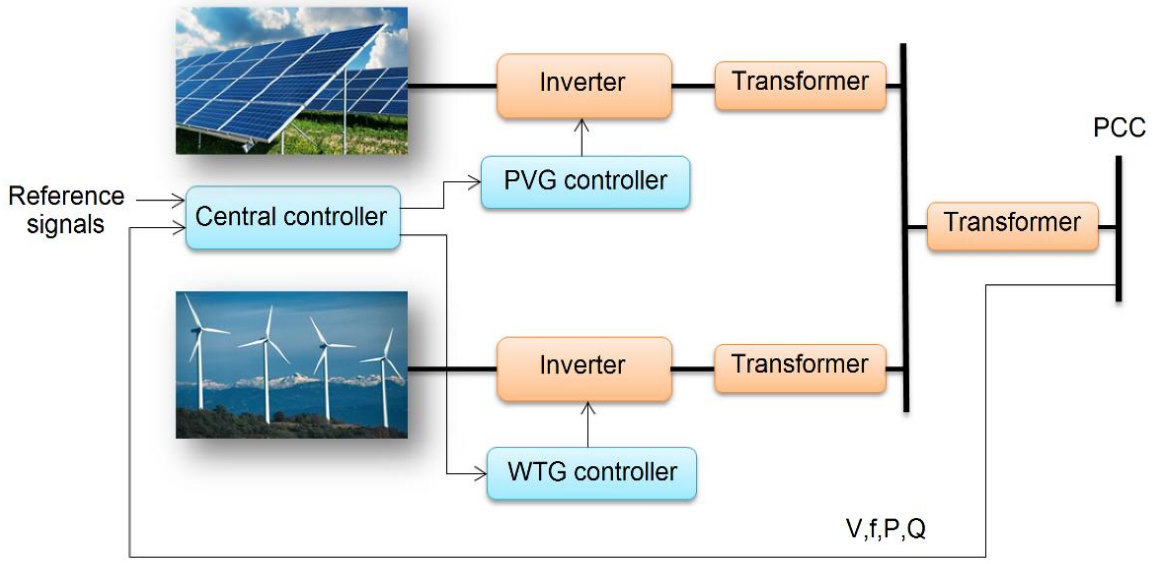

FIGURE 2. General structure of the LWPF.

Given that the converter-based units are connected to the grid by inverters, their dynamic is too fast and can usually be ignored in stability studies. Thus, their converted energy is assumed to be constant [38, 39]. Usually, the inverters of LWPFs are modeled as the current-controlled current sources [38, 39]. In some software packages, this model is available as a static generator. As mentioned, the fourth component of the LWPF is the controllers, which play a fundamental role in the system response during the dynamic conditions. Thus, the modeling of the LWPFs controller is essential to analyze the grid stability.

A. POWER FLOW MODEL

To study the behavior of a power grid, which has an LWPF, it is needed to have a power flow model of the LWPF. As mentioned, the LWPF consists of PVGs and WTGs, each of which includes smaller units. For example, a PVG unit includes many photovoltaic PV panels and inverters. In order to conduct power flow study, the total number of units is necessary to be considered as an equivalent unit in which its rated power is equal to the sum of the rated powers of individual units. This model is called simple aggregated model [38, 39]. As shown in Figure 3, the simple aggregated model can be used for power flow analysis. Also, each unit is considered as a conventional generator for the LWPF, which involves PVG and WTG units. The connecting point to the power system is called point of common coupling (PCC).

B. DYNAMIC MODEL

From the beginning of the development of REPPs, the lack of access to a comprehensive and generic dynamic model has been a major problem in studying the power system stability. First, research models or models created by power plant owners were used [40]. These models had their own problems although they could satisfy the study requirements in many cases.

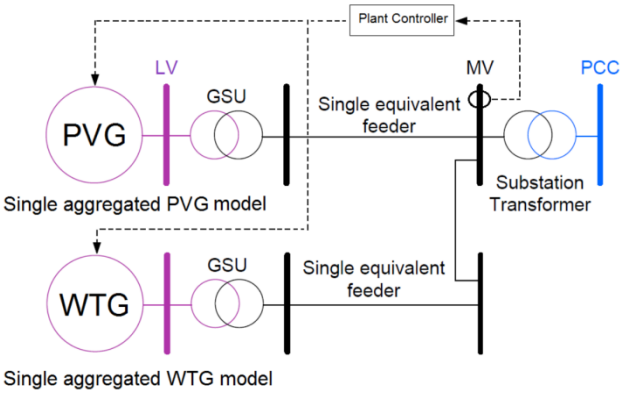

FIGURE 3. Simple aggregated model.

However, the lack of a generic, accessible, and flexible model, which could be used for a variety of REPPs, was evident before expanding the establishment and development of REPPs [38]. Although different models have been presented by well-known companies and institutes later [41–43], the model that introduced by General Electric (GE) and accepted by Western Electricity Coordinating Council (WECC), called first-generation generic model, is regarded as the leading one [41, 42]. Since 2010, WECC has initiated to develop this model for further flexibility and adapt it to a wide range of control strategies for the possibility of modeling different types of equipment for power plants. The result was second generation generic model (SGGM) presented in 2012 [43]. The block diagram of the SGGM is shown in Figure 4.

This article has been accepted for publication in a future issue of this journal, but has not been fully edited. Content may change prior to final publication. Citation information: DOI 10.1109/ACCESS.2021.3094170, IEEE Access

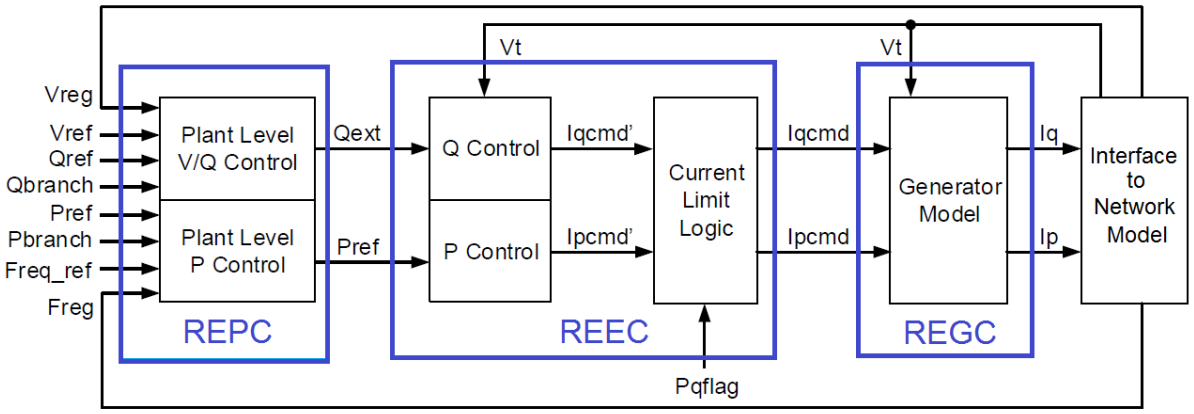

FIGURE 4. **Modular structure of SGGM.**

Due to the increasing tendency to use the hybrid REPPs (HREPPs), WECC and Electric Power Research Institute (EPRI) conducted some studies to present a generic model for this type of power plants. Ultimately, an initial model called generic dynamic model of HREPPs was presented by them [38, 39]. This model, which was based on the SGGM, is currently under development [38]. Generally, these models consist of three basic modules as follows [39]:

- Renewable energy generator/converter (REGC).
- Renewable energy electrical control (REEC).
- Renewable energy plant control (REPC).

The creation of a dynamic model for HREPPs was based on the development of the REPC module. This module is the model of a central controller that sends control signals to other controllers [38, 38]. In other words, in the dynamic model of HREPP, the central controller can send control signals to several different controllers. Figure 3 shows the schematic structure of the REPC module in the dynamic model of HREPP [38]. Therefore, this model can be used to model the LHWPF. As shown in Figure 1, the LWPF consists of three main controllers, a PVG controller, a WTG controller and a central controller. The dynamic model of the LWPF is shown in Figure 5.

It should be noted that the SGGM and the HREPP dynamic model have the ability to model a wide range of inverter-based generators [38, 39]. Therefore, the modules defined in these models have differences according to the generator type, so each of the modules has a specific version. In this study, the versions of REPC, REEC, REGC modules are B, B, and A, respectively [39].

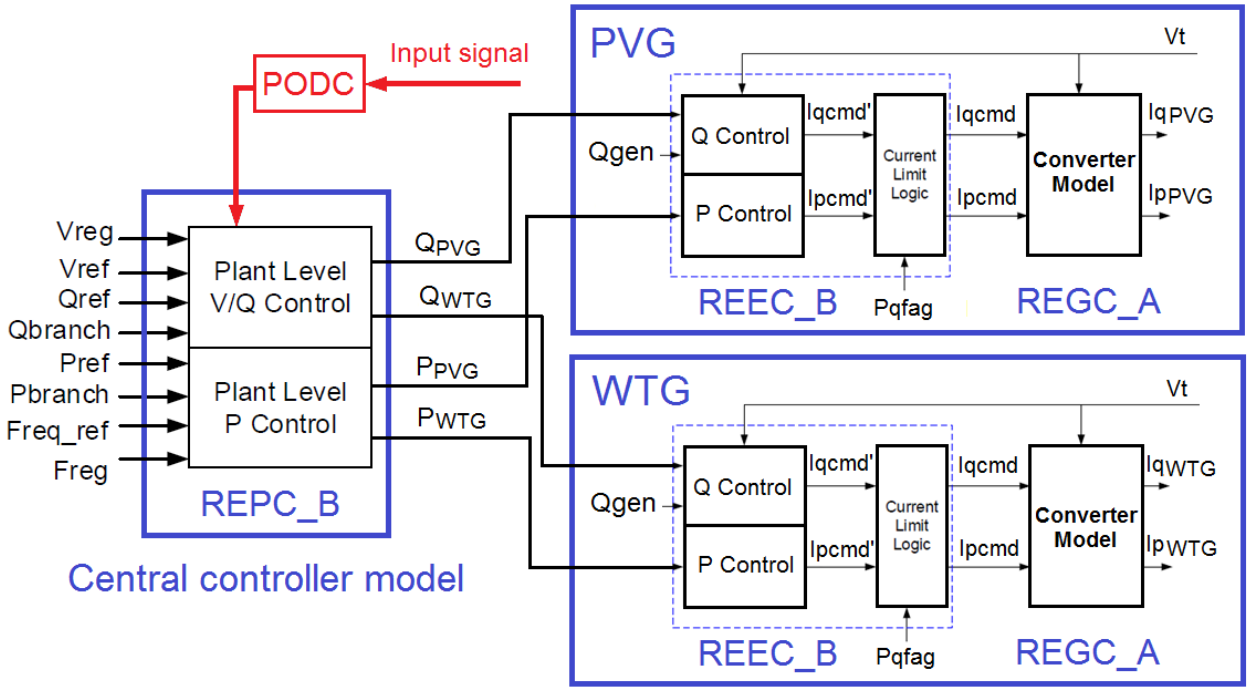

FIGURE 5. **Dynamic model of LWPF.**

This article has been accepted for publication in a future issue of this journal, but has not been fully edited. Content may change prior to final publication. Citation information: DOI 10.1109/ACCESS.2021.3094170, IEEE Access

III. Survey on FOPID controller

The FOPID controllers are based on fractional-order calculus, which is a famous mathematical concept that generalizes conventional integer-order calculus into arbitrary orders. This issue has a history of more than 300 years, yet its application in different fields has been realized only recently due to its implementation complexity in reality [22-30].

Fractional differential equations based on fractional-order calculus have emerged as one of the most important areas of interdisciplinary interest in recent years [20-25]. The fractional-order differentiator, which can be denoted by a general fundamental operator as a general form of differential and integral operators, is defined as follows [22]:

$$ {}_aD_t^q = \begin{cases} \frac{d^q}{dt^q} & , q > 0 \\ 1 & , q = 0 \\ \int_a^t (d\tau)^{-q} & , q < 0 \end{cases} \quad (1) $$

where, q indicates the fractional-order. Also, a and t are the lower and upper limits of D, respectively. Note that q can be a complex number. There are three popular definitions for the fractional-order differentiator, Grunwald Letnikov (GL) definition, Riemann Liouville (RL) definition, and Caputo definition [22]. The GL definition is as follows:

$$ {}_aD_t^q f(t) = \lim_{h \to 0} \frac{1}{h^q} \sum_{j=0}^{[(t-a)/h]} (-1)^j \binom{n}{j} f(t - jh) \quad (2) $$

$$ \binom{n}{j} = \frac{\Gamma(n+1)}{\Gamma(j+1)\Gamma(n-j+1)} \quad (3) $$

where, n is the integer value that satisfies the condition and $n\text{-}1 < q < n$. In addition, Γ function represents the Euler's Gamma function as indicated in (4). Also, operator [ ] in (2) indicates a floor function [22, 25].

$$ \Gamma(x) = \int_0^\infty t^{(x-1)} e^{-t} dt \quad (4) $$

Also, the RL definition is as follows [22, 25]:

$$ {}_aD_t^q f(t) = \frac{1}{\Gamma(n-q)} \frac{d^n}{dt^n} \int_a^t \frac{f(\tau)}{(t-\tau)^{q-n+1}} d\tau \quad (5) $$

where, $n\text{-}1 < q < n$.

Moreover, Caputo presented the definition of fractional differintegral in 1976 as follows [22, 25]:

$$ {}_aD_t^q f(t) = \frac{1}{\Gamma(n-q)} \int_a^t \frac{f^n(\tau)}{(t-\tau)^{q-n+1}} d\tau \quad (6) $$

where, $n\text{-}1 < q < n$.

A. FOPID CONTROLLER

The general form of the PID controller is the FOPID controller. This controller provides higher robustness and stability area than common controllers due to the extra degrees of freedom resulting from the orders of fractional integral λ, and fractional derivative δ [22]. As shown in Figure 6, the FOPID controller is the expansion of the PID controller [22].

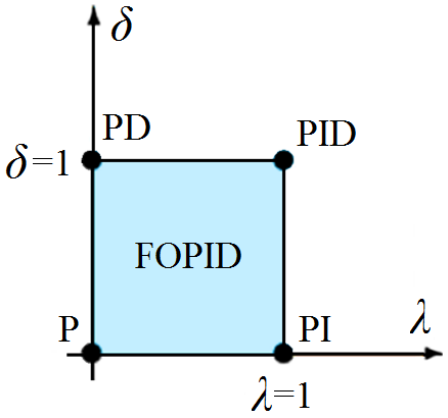

FIGURE 6. Graphical presentation of FOPID controller in δ- λ, plane

The conventional PID controller has three variables (K_P, K_I, and K_D) while the FOPID has five variables (K_P, K_I, K_D, λ, and δ). The ability to manage model uncertainties in non-linear applications, more flexibility in tuning, and high disturbance rejection are other advantages of the FOPID controller [20, 24]. The fractional-differential-equation of this type of controller is expressed as follows [22, 29]:

$$ U(t) = K_P E(t) + K_I D_t^{-\lambda} E(t) + K_D D_t^{\delta} E(t) \quad (7) $$

Also, the transfer function $C(s)$, in Laplace form is as below:

$$ C(s) = \frac{U(s)}{E(s)} = K_P + K_I s^{-\lambda} + K_D s^{\delta} \quad (8) $$

where, $E(s)$ is the input and $U(s)$ is the output. As well as, K_P, K_I and K_D represent the proportional, integral, and derivative gains of the FOPID controller. Moreover, λ and δ display the fractional-orders of integral and derivative. The controller structure has been shown in Figure 7 [22].

This article has been accepted for publication in a future issue of this journal, but has not been fully edited. Content may change prior to final publication. Citation information: DOI 10.1109/ACCESS.2021.3094170, IEEE Access

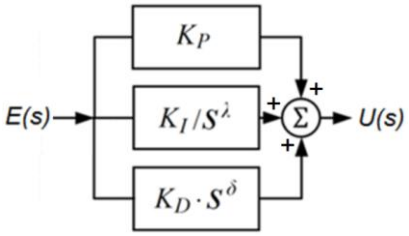

FIGURE 7. Schematic structure of FOPID controller.

B. STABILITY OF FRACTIONAL-ORDER SYSTEMS

The fractional-order systems stability is somewhat different from the integer-order systems, duo to the inherent characteristics of fractional-order calculus. In a stable fractional-order system, the roots may be located in the right side of the imaginary axis.

The state-space model of fractional-order linear-time invariant system is stated as bellow [30, 44]:

$$ {}_0D_h^q\, x(t) = Ax(t) + Bu(t) \quad (9) $$

$$ y(t) = Cx(t) \quad (10) $$

where, $x \in R^n$, $u \in R^m$ and $y \in R^p$ are the state vector, vector of system inputs and vector of system outputs. For an n-th order system with m inputs and p outputs, $A \in R^{n\times n}$, $B \in R^{n\times m}$ and $C \in R^{p\times n}$ are the system matrix, input matrix and output matrix. Also, $q = [q_1, q_2, \dots, q_n]^T$ is the fractional-orders vector. The stability condition for a fractional-order system based on Matignon's Stability Theorem can be presented as bellow [30, 44]:

The fractional-order system in (9) and (10) is stable if and only if:

$$ |arg\,(eig(A))| > (q\,\pi)/2 \quad (11) $$

where, *eig(A)* represents the eigenvalue of matrix *A*. The stability area of fractional-order system depends on the value of q [31, 45]. Given that, in FOPID controllers, the fractional-orders, λ and δ, are between 0 and 1, so this type of controllers has a wide range of stability area as shown in Figure 8.

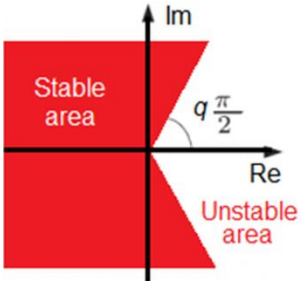

FIGURE 8. Stability area of FOPID controller.

IV. Implementation of PMU-based FOPID-PODC

In this paper, a FOPID controller is suggested to damp LFOs by the LWPF. The FOPID-PODC is implemented in the central controller of the LWPF. Also, the input signals are received from PMUs, so the controller function is based on a WAMS [6, 7].

As indicated in Figure 9, two various points are proposed for the FOPID-PODC in the central controller model called REPC_B model. Each of these points is considered based on the LWPF control mode for reactive power/voltage control. Point 1 is suggested, if the control mode is voltage control. Therefore, the PCC is considered as a PV bus. Moreover, point 2 is suggested, if the reactive power control mode is selected for the LWPF operation mode. So, the PCC is considered as a PQ bus.

V. Case study

To further investigate the issue, it is necessary to evaluate the performance of the proposed controller in a benchmark test system. Therefore, having the necessary information about the power system is necessary for the first step to design the proposed controller.

A. TEST SYSTEM

There are various benchmark grids for LFO studies; the most important and well-known one is the two-area system [45, 46]. In this study, this system with a secure communication infrastructure is considered as a smart grid. As depicted in Figure 10, the LWPF is connected to bus 6. It should be noted that this bus is considered as the PCC. Also, only generator G2 has a PSS in the excitation system. The specifications of the mentioned system are given in Table 1.

As mentioned, the test system has a secure communication infrastructure layer. Therefore, the grid uses a WAMS to measure the desired signals. The required signals are measured by PMUs, connected to the generator buses, and transmitted to the phasor data concentrator (PDC) for data processing. Finally, required signals are sent to the relevant equipment by the WAMS. It is clear that signal transmission has a time delay that needs to be considered in studies. In this paper, the time delay is assumed to be constant. Also, the values of the LWPF parameters, excitation system of synchronous generators, and PSS of generator G2 are given in the appendix. Other data is in accordance with the specifications of the two-area system in [46].

TABLE 1. Characteristics of the test system.

Item	Description/ Value
Generators model	Sixth-order model
LWPF rating	300 MVA
WTG s rating	150 MVA
PVGs rating	150 MVA
Generators rating	G1, G3, G4: 900 MVA , G2: 600 MVA
Exciters model	IEEE type ST1A
PSSs model	Conventional type STAB1 (Only *G2*)
Loads	Constant power load
Load (L1)	967 MW/100 MVAr
Load (L2)	1767 MW/ 100 MVAr
LWPF control mode	Voltage control [47, 48]

This article has been accepted for publication in a future issue of this journal, but has not been fully edited. Content may change prior to final publication. Citation information: DOI 10.1109/ACCESS.2021.3094170, IEEE Access

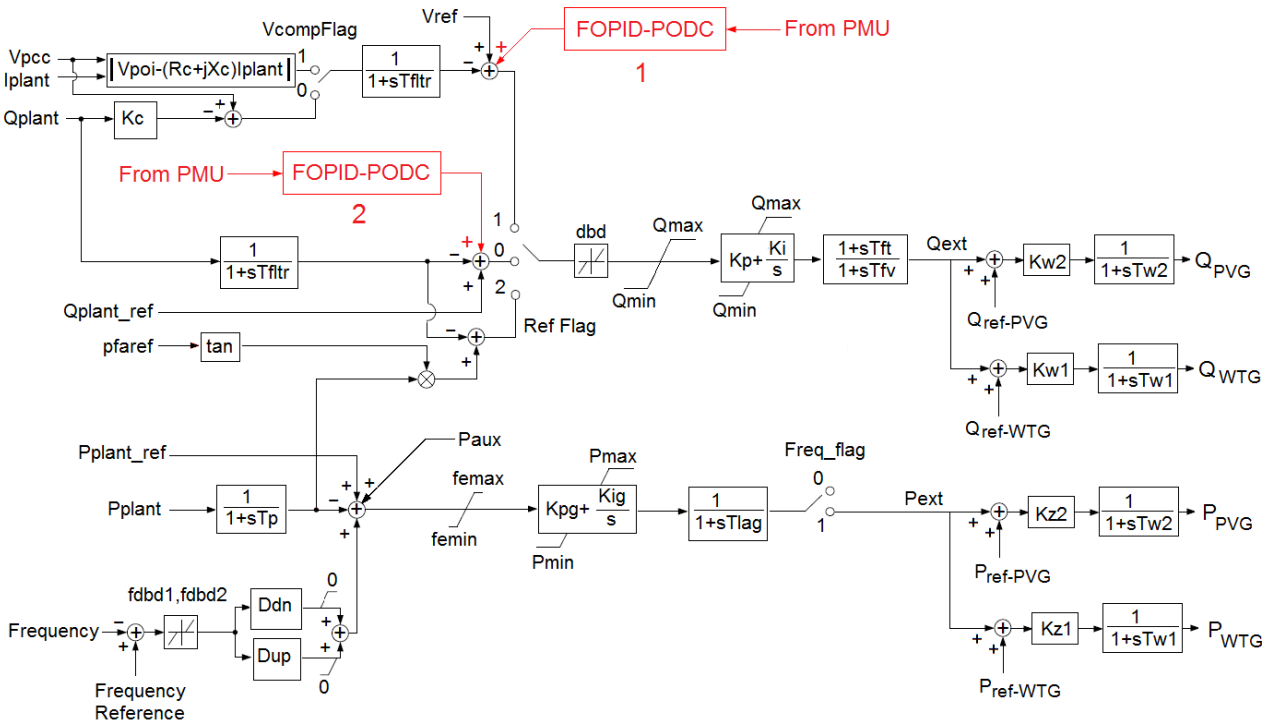

FIGURE 9. Schematic structure of central control model of LWPF (REPC_B) with proposed FOPID-PODC.

In this study, the LWPF control mode for reactive power/ voltage control is defined as voltage control mode [39, 43]. In this mode, the point 1 is considered for the FOPID-PODC. Moreover, governor response mode, up and down regulation, is selected as the active power/frequency control mode. Note that the variation of generators speed across the two areas is considered as the input signal of the FOPID-PODC [47]. Also, the time delay of the signal transmission among PMUs, PDC and FOPID-PODC is considered as constant time delay, T_m , which is 100 ms [48].

B. TUNING OF PMU-BASED FOPID-PODC

One of the most important challenges of the FOPID controllers is their tuning. The presence of fractional-order parameters in the differential equation and a large number of parameters make it impossible to use conventional tuning methods.

So far, two methods have been used for the FOPID controller tuning in different power systems studies. The rule-based methods are based on approximation and numerical methods are based on optimization [49]. The first group is based on the approximation of the fractional-order function to an integer-order function [49]. Another group uses the optimization algorithms by considering an objective function (OF) and determining the optimal values of the parameters [49].

In this paper, the optimization method is used for the controller tuning. So, the FOPID-PODC parameters are determined by solving an optimization problem subjected to technical constraints. For this purpose, an OF based on the integral of the time-weighted absolute error (ITAE) index, is considered as follows [50]:

$$OF = \sum_{L=1}^{N_L} (ITAE) \tag{12}$$

where, N_L denotes the number of loading conditions. Also, the ITAE index is as follows:

$$ITAE = \int_0^{t_{sim}} t.|e(t)|\ dt \tag{13}$$

where, t presents the time variable and t_{sim} denotes the simulation time, which is 20 s in this paper [51]. In addition, *e(t)* is the error function. Note that there are several generators in the smart grid, so, the OF should consider the effect of all of them [52]. For this purpose, the sum of the speed deviation of the generators is considered as an error function, as follows [50, 52]:

$$|e(t)| = \sum_{G=1}^{n_G} |\Delta\omega_G(t)| \tag{14}$$

where, n_G indicates the number of grid generators and $\Delta\omega_G$ indicates the speed deviation of the generator *G*. The optimization is implemented by applying a large disturbance to the test system for three loading conditions. Therefore, a three-phase short circuit event at bus 8 is considered for 100 ms; because this event creates the most severe short-circuit current in the transmission lines of the test system. Table 2 presents the loading conditions. Note that the loading

This article has been accepted for publication in a future issue of this journal, but has not been fully edited. Content may change prior to final publication. Citation information: DOI 10.1109/ACCESS.2021.3094170, IEEE Access

conditions are considered based on steady-state stability. For optimal adjustment of the FOPID-PODC, (12) must be minimized subject to parameters constraints listed in Table 3.

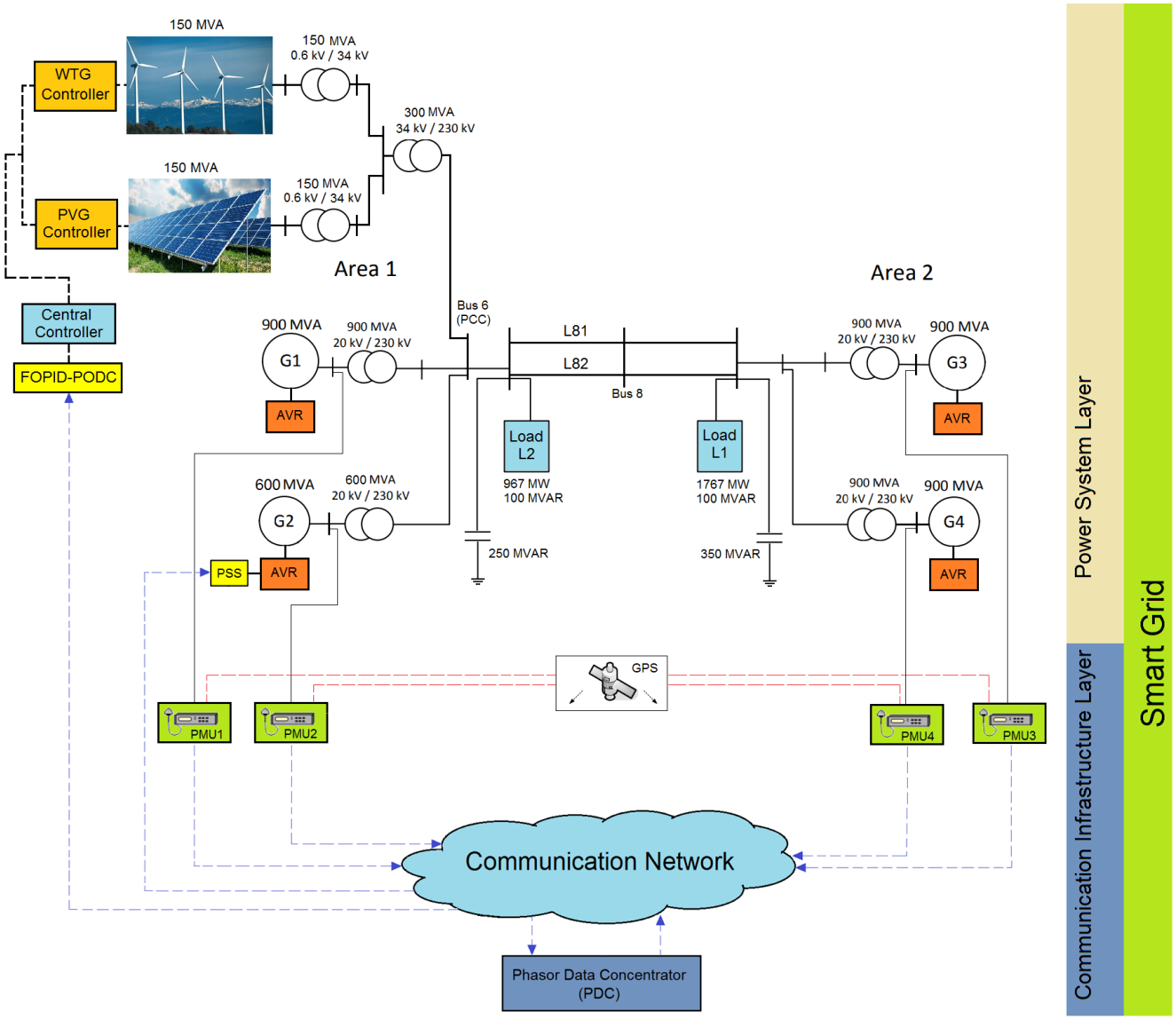

FIGURE 10. Smart two-area test system with LWPF.

TABLE 2. Loading conditions.

Item	System loading (%)
Condition 1	100
Condition 2	90
Condition 3	110

TABLE 3. Constraints of the FOPID-PODC parameters.

Item	K_P	K_I	K_D	δ	λ
Upper band	100	100	100	1	1
Lower band	0	0	0	0	0

In this study, the TLBO algorithm is used for optimal tuning of the proposed controller [53, 54]. The optimization process is in accordance with the flowchart in Figure 11.

Also, Particle swarm optimization (PSO) algorithm and genetic algorithm (GA) were used to compare the results [55, 56]. The results of the implementation of optimization algorithms are shown in Figure 12. As shown in this figure, the best value of the OF is obtained by the TLBO. Table 4 lists the best values of the OF obtained by the three algorithms. Also, Table 5 presents the optimal values of the FOPID-PODC parameters based on TLBO.

This article has been accepted for publication in a future issue of this journal, but has not been fully edited. Content may change prior to final publication. Citation information: DOI 10.1109/ACCESS.2021.3094170, IEEE Access

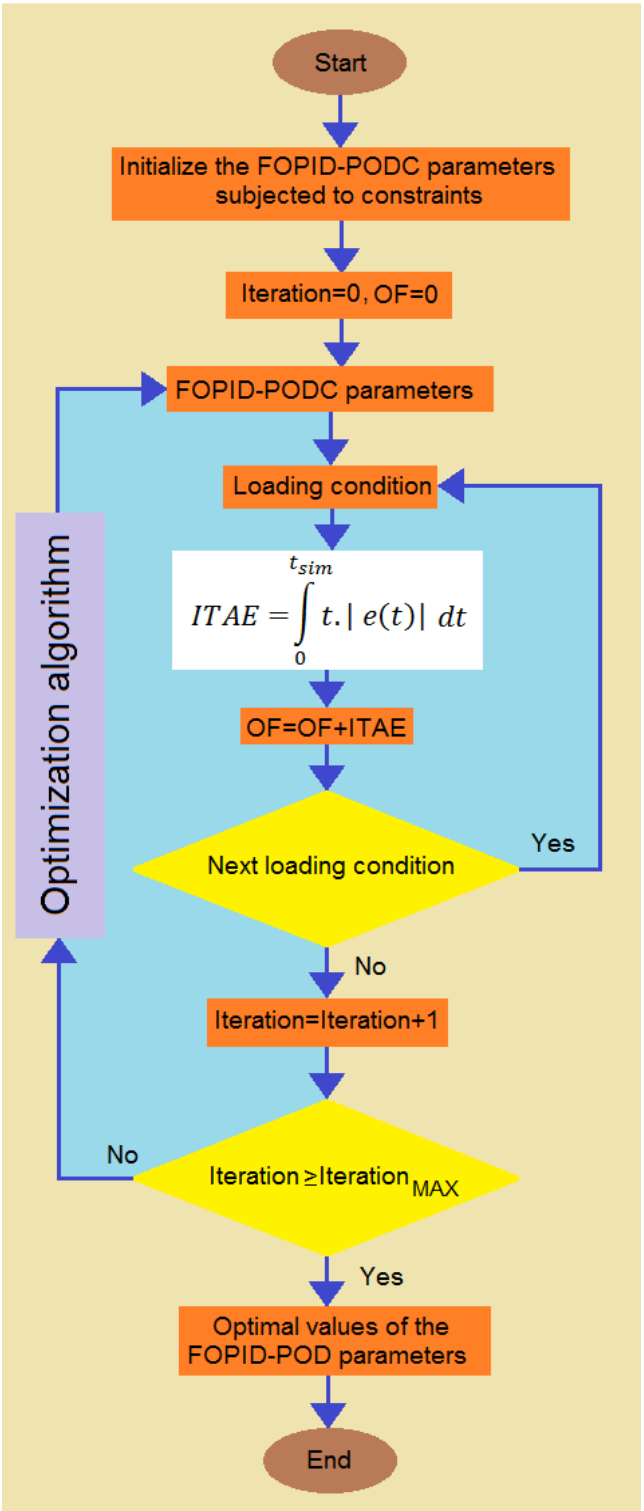

FIGURE 11. Optimization flowchart.

TABLE 4. Best value of the OF for three algorithms.

Algorithm	Best value of the OF
TLBO	0.127836
PSO	0.127925
GA	0.129011

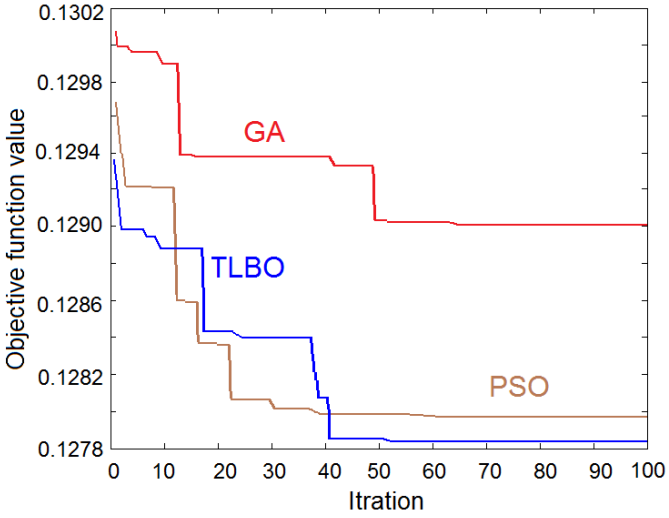

FIGURE 12. OF convergence.

TABLE 5. Optimal values of the FOPID parameters based on TLBO

Parameter	Optimal value
K_P	55.525
K_I	20.174
K_D	76.314
δ	0.267
λ	0.153

C. SIMULATION AND PERFORMANCE EVALUATION

In this section, scenarios are presented to evaluate the performance of the FOPID-PODC. The scenarios have been defined in such a way that they cause the LFOs in the grid. However, the severity of events is not the same. Note that, in conventional power systems, these events are caused by natural or technical reasons. In smart grids, system hacking and cyber-attacks can also cause these events. The scenarios are listed in Table 6.

TABLE 6. Proposed scenarios for performance evaluation.

Scenario	Event	Duration
1	3-Phase fault at bus 8	150 ms
2	Outage of generator *G1*	100 ms
3	Outage of tie-line *L81*	150 ms
4	Outage of load *L1*	100 ms

To analyze the controller performance to damp the LFOs, the four mentioned scenarios are simulated for two modes with and without controller. The results are depicted in Figures 13 to 16.

As the simulation results indicate, the proposed controller has a good effect on LFOs damping. The results also show that the FOPID-PODC damps the frequency and voltage oscillations well.

This article has been accepted for publication in a future issue of this journal, but has not been fully edited. Content may change prior to final publication. Citation information: DOI 10.1109/ACCESS.2021.3094170, IEEE Access

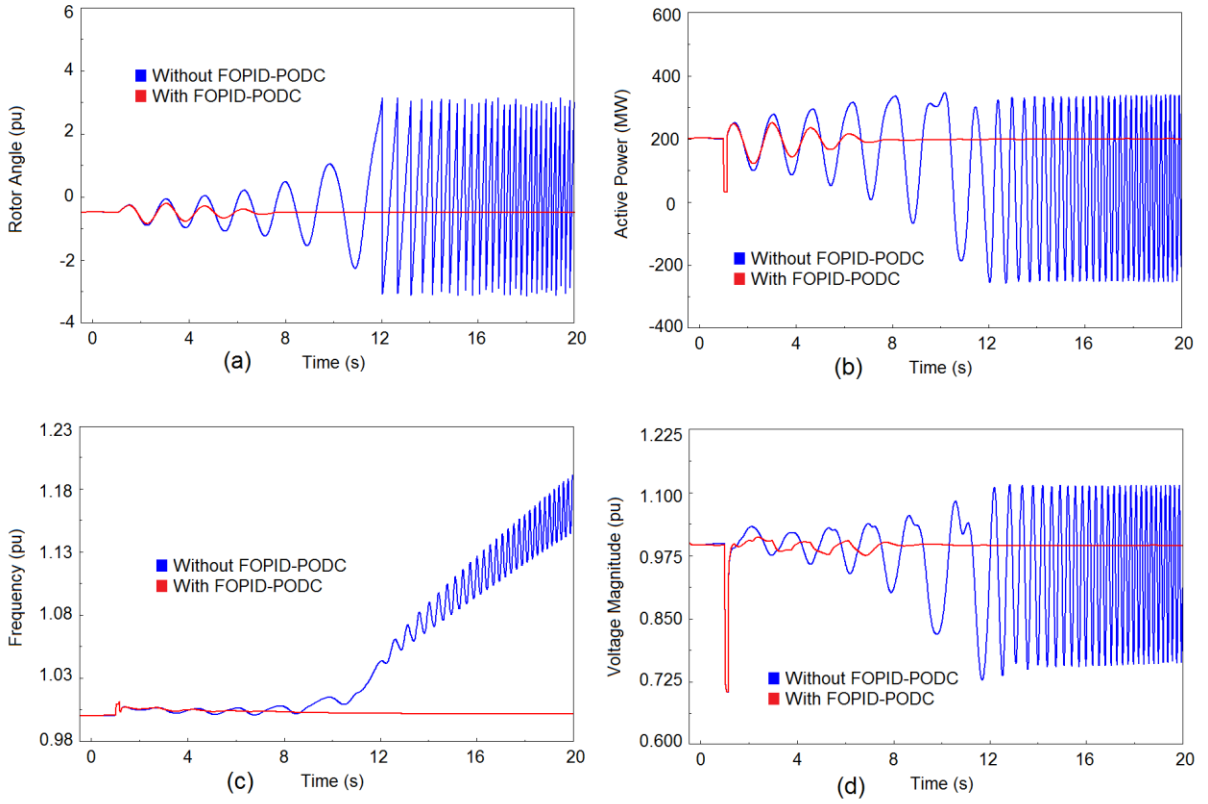

FIGURE 13. Scenario 1; (a) rotor angle of generator *G1*, (b) active power of line *L82*, (c) PCC frequency, and (d) voltage magnitude of the PCC.

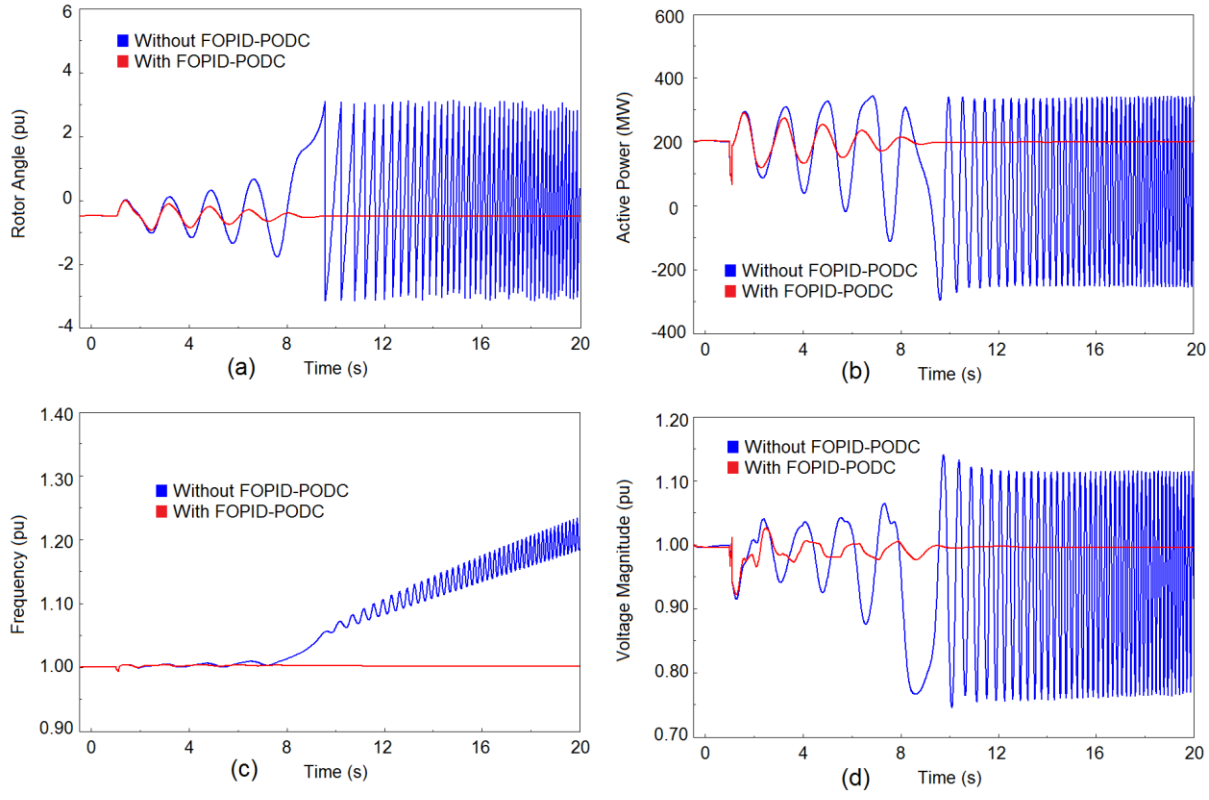

FIGURE 14. Scenario 2; (a) rotor angle of generator *G1*, (b) active power of line *L82*, (c) PCC frequency, and (d) voltage magnitude of the PCC.

This article has been accepted for publication in a future issue of this journal, but has not been fully edited. Content may change prior to final publication. Citation information: DOI 10.1109/ACCESS.2021.3094170, IEEE Access

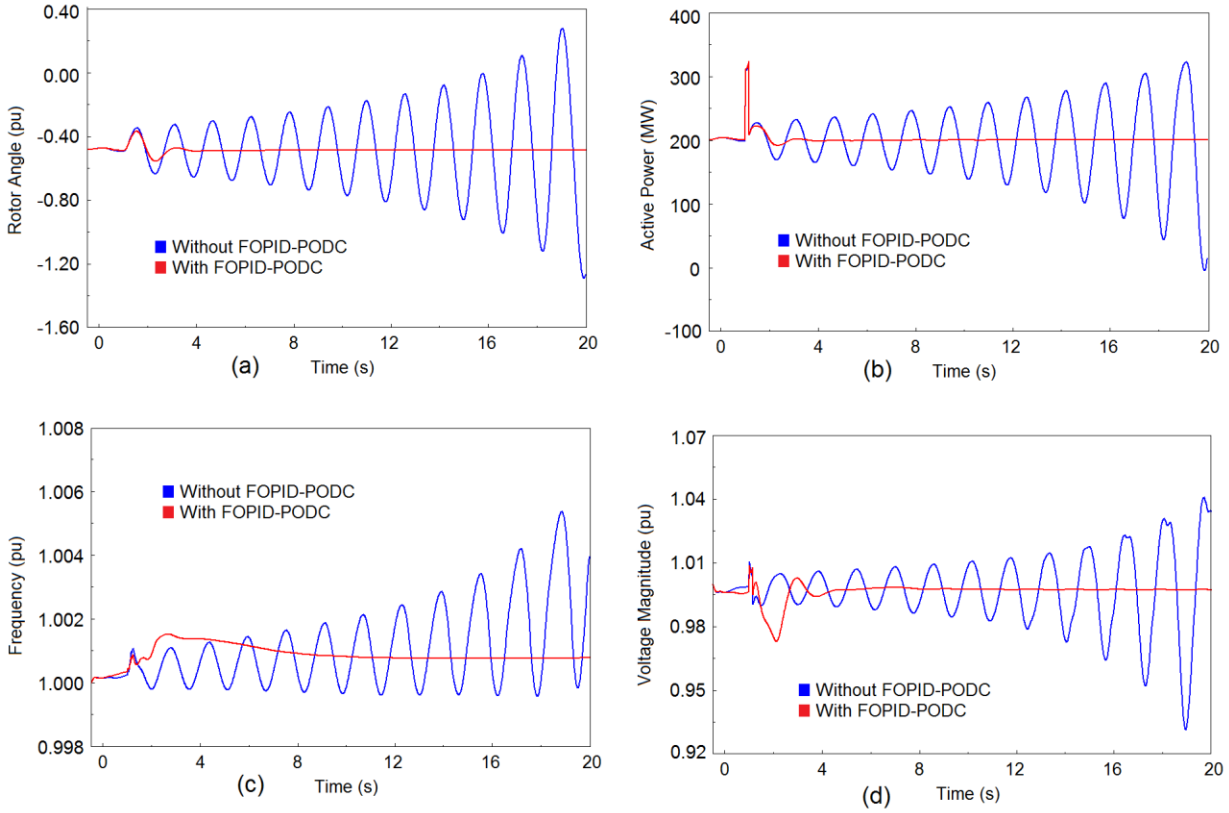

FIGURE 15. Scenario 3; (a) rotor angle of generator *G1*, (b) active power of line *L82*, (c) PCC frequency, and (d) voltage magnitude of the PCC.

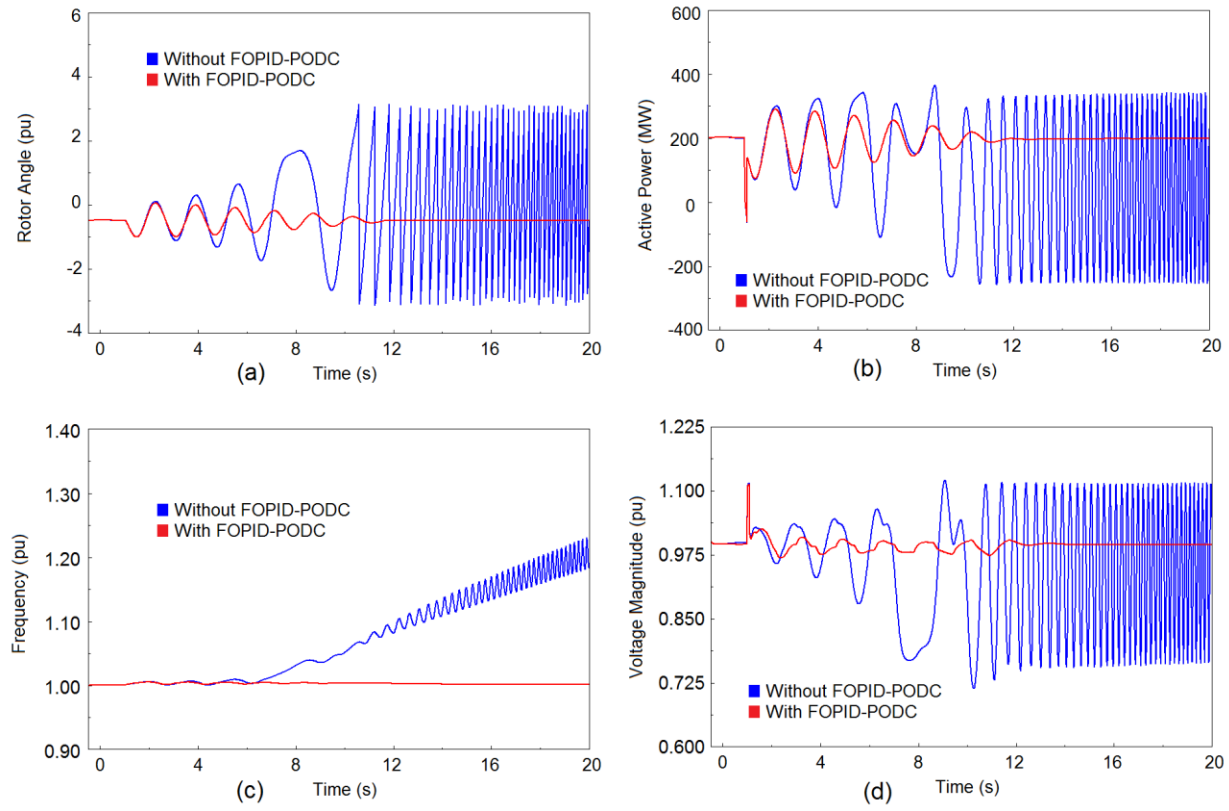

FIGURE 16. Scenario 4; (a) rotor angle of generator *G1*, (b) active power of line *L82*, (c) PCC frequency, and (d) voltage magnitude of the PCC.

This article has been accepted for publication in a future issue of this journal, but has not been fully edited. Content may change prior to final publication. Citation information: DOI 10.1109/ACCESS.2021.3094170, IEEE Access

1) GENERATION UNCERTAINTY OF LWPF

As mentioned in the introduction, one of the main challenges of REPPs is their production uncertainty [2, 3]. Although using the LWPF reduces this uncertainty, it cannot be ignored. Therefore, the performance of the LWPF for LFOs damping should be examined in conditions where the power generation is less than the nominal capacity. Accordingly, in this subsection, the scenarios are simulated in several different capacities and the performance of the FOPID-PODC is evaluated for LFOs damping. The results are depicted in Figures 17 to 20. As the simulation results indicate, despite the reduction in the LWPF generation capacity, there is the necessary to damp the LFOs and the proposed FOPID-PODC is effective.

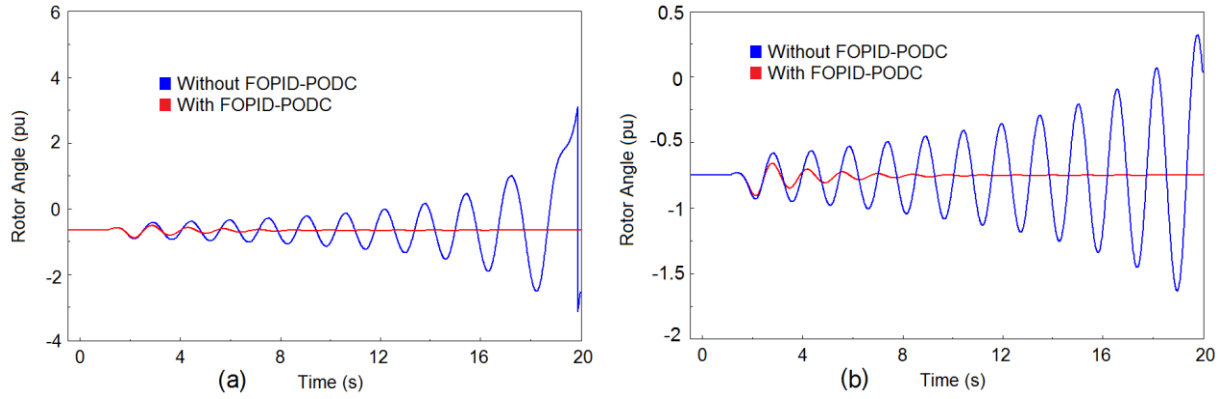

FIGURE 17. Rotor angle of generator *G1* for various capacities of LWPF for scenario 1; (a) 50% and (b) 25% of nominal capacity.

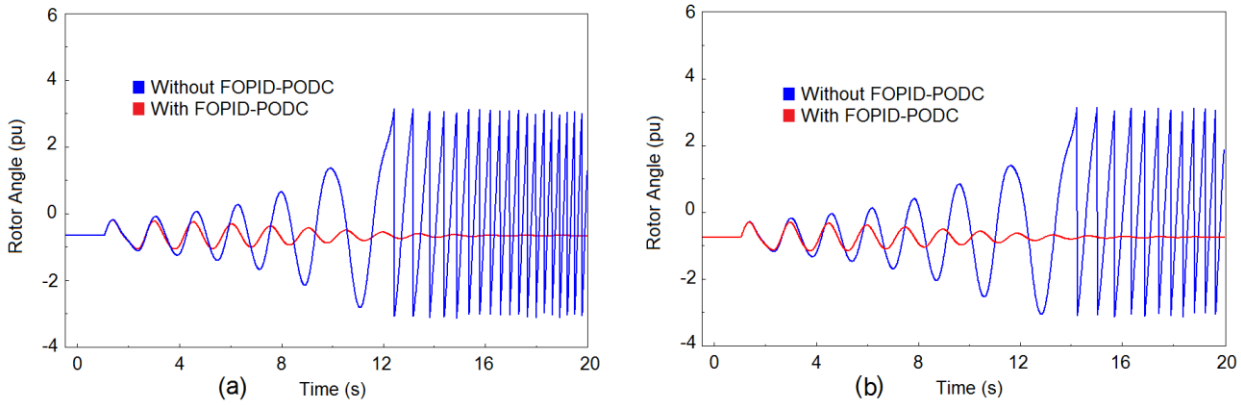

FIGURE 18. Rotor angle of generator *G1* for various capacities of LWPF for scenario 2; (a) 50% and (b) 25% of nominal capacity.

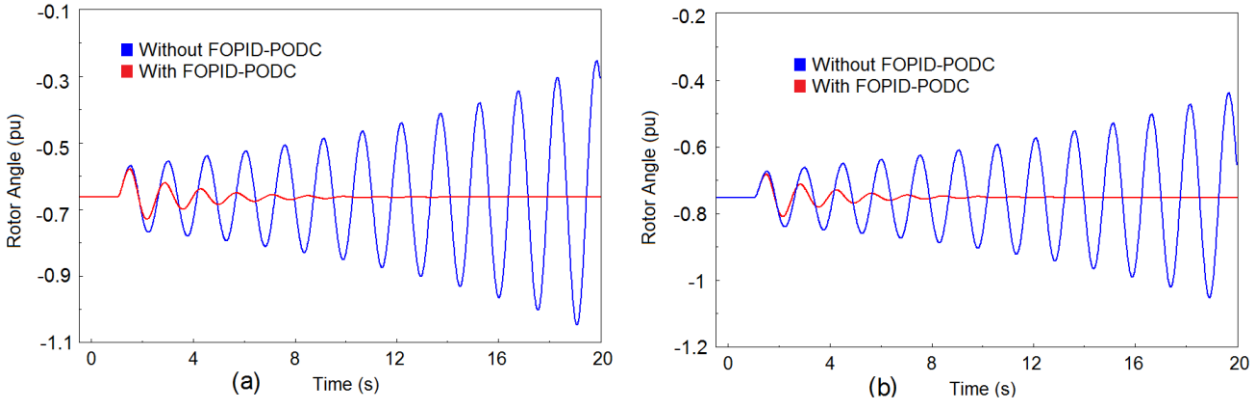

FIGURE 19. Rotor angle of generator *G1* for various capacities of LWPF for scenario 3; (a) 50% and (b) 25% of nominal capacity.

This article has been accepted for publication in a future issue of this journal, but has not been fully edited. Content may change prior to final publication. Citation information: DOI 10.1109/ACCESS.2021.3094170, IEEE Access

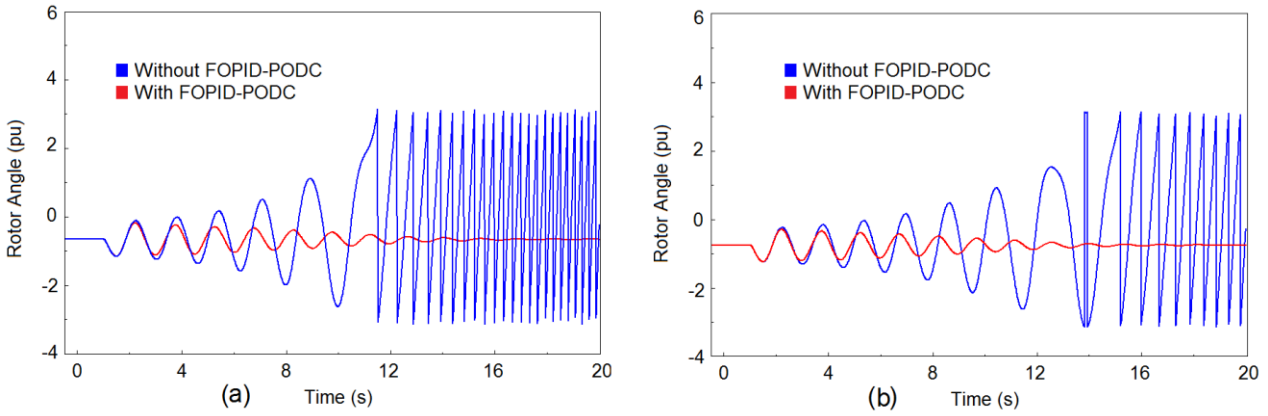

FIGURE 20. Rotor angle of generator *G1* for various capacities of LWPF for scenario 4; (a) 50% and (b) 25% of nominal capacity.

2) UNCERTAINTY OF TIME DELAY OF INPUT SIGNAL

One case, which must be considered in smart grids, is time delay of communication signals. Although with the development of communication infrastructures and the creation of new technologies in ICT, the amount of time delay is reduced, it cannot be ignored, as shown in Table 7 [57].

The time delay of the FOPID input signal may cause the controller malfunction [58]. To avoid this problem, the controller must have the necessary robustness against time delay uncertainty. In this subsection, the robustness of the FOPID-PODC of the LWPF in various time delays is investigated. As indicated in Figure 21, the proposed FOPID-PODC shows high robustness against different time delays of the input signal in four scenarios.

TABLE 7. Time delay of various communication links [52].

Communication link	Time delay (ms)
Fiber optic cable	100-150
Microwave link	100-150
Power line carrier (PLC)	150-350
Telephone line	200-300
Satellite link	500-700

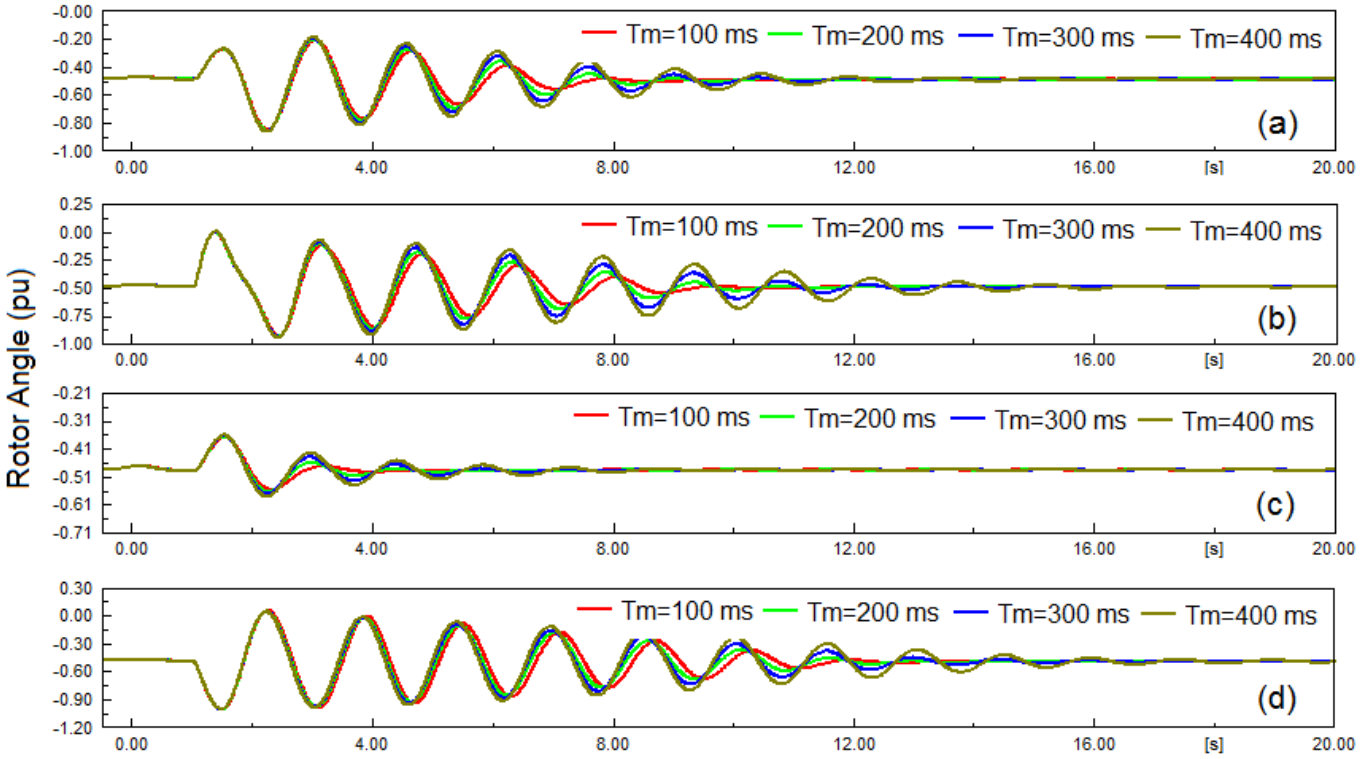

FIGURE 21. Rotor angle of generator *G1* for various time delays of input signal; (a) scenario 1, (b) scenario 2, (c) scenario 3, and (d) scenario 4.

This article has been accepted for publication in a future issue of this journal, but has not been fully edited. Content may change prior to final publication. Citation information: DOI 10.1109/ACCESS.2021.3094170, IEEE Access

3) UNCERTAINTY OF SYSTEM LOADING

One of the most important uncertainties of power systems is system loading, which can affect the proper performance of equipment. Switching, relocating system loads, and outage of loads as well as adding new loads to the system are issues that undermine the certainty of the power system loading condition. Accordingly, it is necessary that the proposed FOPID-PODC has sufficient robustness against this type of uncertainty. So, the performance evaluation of the FOPID-PODC under different system loadings is required. As indicated in Figure 22, the proposed FOPID-PODC shows high robustness against 10% variation in system loading for four scenarios.

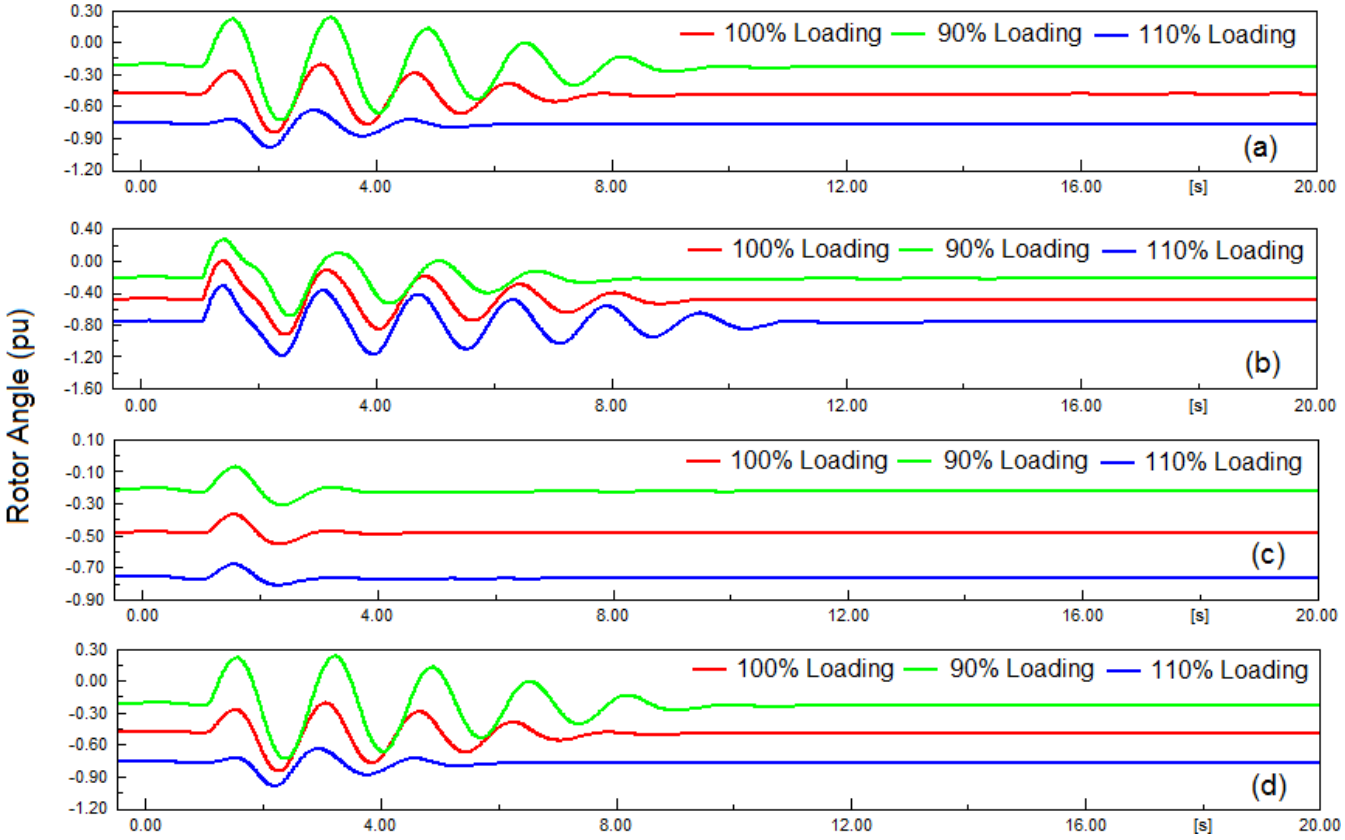

FIGURE 22. **Rotor angle of generator *G1* for various system loadings; (a) scenario 1, (b) scenario 2, (c) scenario 3, and (d) scenario 4.**

The results show the proper performance of LWPF to damp the LFOs. It can also be concluded that the proposed FOPID-PODC controller has sufficient robustness to some smart grid uncertainties.

VI. Conclusion

In smart grids, there is a great demand for electrical power generation by REPPs. In fact, the integration of REPPs is the foundation of future power systems. Despite all advantages of the REPPs, the uncertainty of electricity generation and generation fluctuations are the main challenges in the operation of this type of power plants. One way to meet this challenge, is to use LWPFs. This paper showed that with the widespread use of LWPFs around the world, these types of REPPs can well damp the LFO of modern power systems that is one of the main tasks of synchronous generators. For this purpose, in this paper, a PMU-based FOPID-PODC was proposed, which showed good performance in simulations compared to the conventional controllers.

APPENDIX

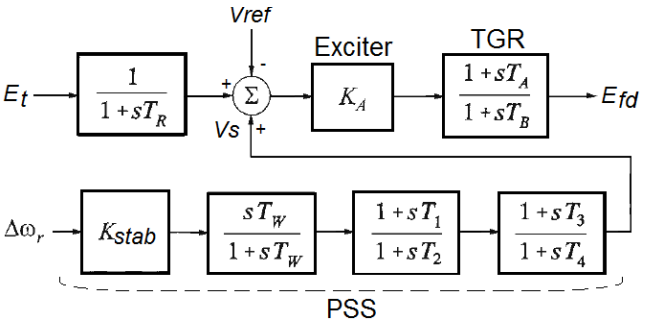

FIGURE 23. **Exciter system of generator with PSS.**

This article has been accepted for publication in a future issue of this journal, but has not been fully edited. Content may change prior to final publication. Citation information: DOI 10.1109/ACCESS.2021.3094170, IEEE Access

TABLE 8. Parameters of the generator exciter.

Name	Description	Value
K_A	Gain	200
T_R	Mesearment delay (s)	0.01
T_A	Derivative time constant	1
T_B	Delay time constant	10

TABLE 9. Parameters of the PSS of generator G2.

Name	Description	Value
Kstab	PSS Gain	65.327
T1	First Lead/Lag derivative time constant	2.769
T2	First Lead/Lag delay time constant	4.593
T3	Second Lead/Lag derivative time constant	3.386
T4	Second Lead/Lag delay time constant	1.1
Tw	Washout integrate time constant	10

TABLE 10. REGC_A parameters in LWPF model.

Name	Description	Value
Tfltr	Terminal voltage filter time constant (s)	0.02
Lvpl1	LVPL gain breakpoint (pu current on mbase / pu voltage)	1.3
Zerox	LVPL zero crossing (pu voltage)	0.4
Brkpt	LVPL breakpoint (pu voltage)	0.9
Lvplsw	low voltage power logic (Enable 1 or disable 0)	0
rrpwr	Active current up-ramp rate limit on voltage recovery (pu/s)	10.0
Tg	Inverter current regulator lag time constant (s)	0.02
Volim	Voltage limit for high voltage clamp logic (pu)	1.2
Iolim	Current limit for high voltage clamp logic (pu on mbase)	-1.3
Khv	High voltage clamp logic acceleration factor	0.7
lvpnt0	Low voltage active current management breakpoint (pu)	0.4
lvpnt1	Low voltage active current management breakpoint (pu)	0.8
Iqrmax	Maximum rate-of-change of reactive current (pu/s)	999
Iqrmin	Minimum rate-of-change of reactive current (pu/s)	-999

TABLE 11. REEC_B parameters in LWPF model.

Name	Description	Value
PFflag	Constant Q (0) or PF (1) local control	0
Vflag	Local Q (0) or voltage control (1)	1
Qflag	Bypass (0) or engage (1) inner voltage regulator loop	0
Pqflag	Priority to reactive current (0) or active current (1)	0
Trv	Terminal bus voltage filter time constant (s)	0.02
Vdip	Low voltage condition trigger voltage (pu)	0
Vup	High voltage condition trigger voltage (pu)	1.3
Vref0	Reference voltage for reactive current injection (pu)	0
dbd1	Overvoltage deadband for reactive current injection (pu)	-0.02
dbd2	Undervoltage deadband for reactive current injection (pu)	0.02
Kqv	Reactive current injection gain (pu/pu)	0
Iqhl	Maximum reactive current injection (pu on mbase)	1.05
Iqll	Minimum reactive current injection (pu on mbase)	-1.05
Tp	Active power filter time constant (s)	0.02
Qmax	Maximum reactive power when Vflag = 1 (pu on mbase)	0.4
Qmin	Minimum reactive power when Vflag = 1 (pu on mbase)	-0.4
Kqp	Local Q regulator proportional gain (pu/pu)	1
Kqi	Local Q regulator integral gain (pu/pu-s)	10
Vmax	Maximum voltage at inverter terminal bus (pu)	1.1
Vmin	Minimum voltage at inverter terminal bus (pu)	0.9
Kvp	Local voltage regulator proportional gain (pu/pu)	0
Kvi	Local voltage regulator integral gain (pu/pu-s)	40
Tiq	Reactive current regulator lag time constant (s)	0.02
Tpord	Inverter power order lag time constant (s)	0.02
Pmax	Maximum active power (pu on mbase)	1.0
Pmin	Minimum active power (pu on mbase)	0.0
dPmax	Active power up-ramp limit (pu/s on mbase)	999
dPmin	Active power down-ramp limit (pu/s on mbase)	0
Imax	Maximum apparent current (pu on mbase)	1.25

TABLE 12. REPC_B parameters in LWPF model.

Name	Description	Value
RefFlag	Plant level reactive power (0) or voltage control (1)	1
VcompFlag	Reactive droop (0) or line drop compensation (1)	1
Freq_flag	Governor response (disable 0 or enable 1)	1
Tfltr	Voltage and reactive power filter time constant (s)	0.02
Rc	Line drop compensation resistance (pu on mbase)	0
Xc	Line drop compensation reactance (pu on mbase) when VcompFlag = 1	0
Kc	Reactive droop (pu on mbase) when VcompFlag = 0	0.02
dbd	Reactive power deadband (pu on mbase) when RefFlag = 0; and Voltage deadband (pu) when RefFlag = 1	0
emax	Maximum V/Q error (pu)	0.1

This article has been accepted for publication in a future issue of this journal, but has not been fully edited. Content may change prior to final publication. Citation information: DOI 10.1109/ACCESS.2021.3094170, IEEE Access

emin	Minimum V/Q error (pu)	-0.1
Kp	V/Q regulator proportional gain (pu/pu)m	1
Kq	V/Q regulator integral gain (pu/pu-s)	10
Qmax	Maximum plant reactive power command (pu on mbase)	0.4
Qmin	Minimum plant reactive power command (pu on mbase)	-0.4
Vfrz	Voltage for freezing V/Q regulator integrator (pu)	0
Tft	Plant controller Qoutput lead time constant (s)	0
Tfv	Plant controller Qoutput lag time constant (s)	0.1
fdbd1	Overfrequency deadband for governor response (pu)	0
fdbd2	Underfrequency deadband for governor response (pu)	0
Ddn	Down regulation droop (pu power/pu freq on mbase)	20
Dup	Up regulation droop (pu power/pu freq on mbase)	10
Tp	Active power filter time constant (s)	0.02
femax	Maximum power error in droop regulator (pu on mbase)	999
femin	Minimum power error in droop regulator (pu on mbase)	-999
Kpg	Droop regulator proportional gain (pu/pu)	1
Kig	Droop regulator integral gain (pu/pu-s)	10
Pmax	Maximum plant active power command (pu on mbase)	1
Pmin	Minimum plant active power command (pu on mbase)	0
Tlag	Plant controller Poutput lag time constant (s)	0.1

REFERENCES

[1] E. Kabalci, "Design and analysis of a hybrid renewable energy plant with solar and wind power," *Energy Conversion and Management,* vol. 72, pp. 51-59, 2013.

[2] M. M. Samy, M. I. Mosaad, M. F. El-Naggar, S. Barakat, "Reliability support of undependable grid using green energy systems: Economic study," *IEEE Access*, vol. 9, pp. 14528-14539, 2020.

[3] A. A. Tawfiq, et al., "Optimal Reliability Study of Grid-Connected PV Systems Using Evolutionary Computing Techniques," *IEEE Access*, vol. 9, pp. 42125-42139, 2021.

[4] J. Quintero, V. Vittal, G. T. Heydt, H. Zhang, "The impact of increased penetration of converter control-based generators on power system modes of oscillation," *IEEE Transactions on Power Systems*, vol. 29, no. 5, pp. 2248-2256, 2014.

[5] R. Shah, N. Mithulananthan, R. C. Bansal, V. K. Ramachandaramurthy, "A review of key power system stability challenges for large-scale PV integration," *Renewable and Sustainable Energy Reviews*, vol. 41, pp. 1423-1436, 2015.

[6] Y. Kabalci, "A survey on smart metering and smart grid communication," *Renewable and Sustainable Energy Reviews*. vol. 57, pp. 302-318, 2016.

[7] M. Faheem, et al. , "Smart grid communication and information technologies in the perspective of Industry 4.0: Opportunities and challenges," *Computer Science Review*. vol. 30, pp. 1-30, 2018.

[8] V. Khare, S. Nema, P. Baredar, "Solar–wind hybrid renewable energy system: A review," *Renewable and Sustainable Energy Reviews*. vol. 58, pp. 23-33, 2016.

[9] K. Anoune, M. Bouya, A. Astito, AB. Abdellah, "Sizing methods and optimization techniques for PV-wind based hybrid renewable energy system: A review," *Renewable and Sustainable Energy Reviews*. vol. 93, pp. 652-673, 2018.

[10] S. Eftekharnejad, V. Vittal, G. T. Heydt, B. Keel, J. Loehr, "Impact of increased penetration of photovoltaic generation on power systems," *IEEE Transactions on Power Systems*, vol. 28, no. 2, pp. 893-901, 2012.

[11] Y. Zhang, S. Zhu, R. Sparks, I. Green, "Impacts of solar PV generators on power system stability and voltage performance," in *2012 IEEE Power and Energy Society General Meeting*, San Diego, CA, pp. 1-7, 2012.

[12] R. Tonkoski, D. Turcotte, T. H. El-Fouly, "Impact of high PV penetration on voltage profiles in residential neighborhoods," *IEEE Transactions on Sustainable Energy*, vol. 3, no. 3, pp. 518-527, 2012.

[13] R. Shah, N. Mithulananthan, A. Sode-Yome, K. Y. Lee, "Impact of large-scale PV penetration on power system oscillatory stability," In *IEEE Power and Energy Society General Meeting*, Minneapolis, MN, USA, pp. 1-7, 2010.

[14] M. Saadatmand, et al., "Damping of Low-Frequency Oscillations in Power Systems by Large-Scale PV Farms: A Comprehensive Review of Control Methods," *IEEE Access*, vol. 9, pp. 72183-72206, 2021.

[15] R. Shah, N. Mithulananathan, K. Y. Lee, "Design of robust power oscillation damping controller for large-scale PV plant," In *2012 IEEE Power and Energy Society General Meeting*, pp. 1-8, 2012.

[16] M. Saadatmand, B. Mozafari, G. B. Gharehpetian, S. Soleymani, "Optimal PID controller of large-scale PV farms for power systems LFO damping," *International Transactions on Electrical Energy Systems*, vol. 30, no. 6, e12372, 2020.

[17] R. Shah, N. Mithulananthan, K. Y. Lee, "Large-scale PV plant with a robust controller considering power oscillation damping," *IEEE Transactions on Energy Conversion*, vol. 28, pp. 106-116, 2012.

[18] L. Zhou, X. Yu, B. Li, C. Zheng, J. Liu, Q. Liu, K. Guo, "Damping Inter-Area Oscillations with Large-Scale PV Plant by Modified Multiple-Model Adaptive Control Strategy," *IEEE Transactions on Sustainable Energy*, vol. 8, pp. 1629-1636, 2017.

[19] M. Singh M, et al., "Interarea oscillation damping controls for wind power plants," *IEEE Transactions on sustainable energy*, vol. 6, no. 3, pp. 967-975, 2015.

[20] J. L. Domínguez-García, O. Gomis-Bellmunt, F. D. Bianchi, A. Sumper, "Power oscillation damping supported by wind power: A review," *Renewable and Sustainable Energy Reviews*. vol. 16, no. 7, pp. 4994-5006, 2012.

[21] M. Saadatmand, B. Mozafari, G. B. Gharehpetian,S. Soleymani, "Damping of low-frequency oscillation in power systems using hybrid renewable energy power plants," *Turkish Journal of Electrical Engineering & Computer Sciences*. vol. 27, no. 5, pp. 3852-3867. 2019.

[22] P. Shah, S. Agashe, "Review of fractional PID controller," *Mechatronics*, vol. 38, pp. 29-41, 2016.

[23] A. Tepljakov, Fractional-order modeling and control of dynamic systems. Ph.D. Dissertation, Tallinn University of Technology, Tallinn, Estonia, 2017.

[24] D. Sibtain, et al. , "Multi control adaptive fractional order PID control approach for PV/wind connected grid system," *International Transactions on Electrical Energy Systems.* vol. 31, no. 4, e12809, 2021.

[25] R. Pradhan, S. K. Majhi, J. K. Pradhan, B. B. Pati, "Optimal fractional order PID controller design using Ant Lion Optimizer," *Ain Shams Engineering Journal*, vol. 11, no. 2, pp. 281-291, 2020.

[26] K. S. Miller, B. Ross, "*An Introduction to the fractional calculus and fractional differential equations*", New York: John Wiley, 1993.

[27] H. Singh, D. Kumar, D. Baleanu, "*Methods of mathematical modelling: fractional differential equations*," Boca Raton, FL: CRC Press, Taylor & Francis Group, 2020.

[28] K. B. Oldham, J. Spanier, "*The fractional calculus*," New York: Academic Press, 1974.

[29] I. Podlubny, Fractional-order systems and PI/sup /spl lambda//D/sup /spl mu//-controllers," *IEEE Transactions on Automatic Control*, vol. 44, no. 1, pp. 208-214, 1999.

[30] C. A. Monje, Y. Chen, B. M. Vinagre, D. Xue, V. Feliu-Batlle, "*Fractional-order systems and controls: fundamentals and applications*", London: Springer Science & Business Media; 2010.

[31] J. Morsali, K. Zare, MT. Hagh, "A novel dynamic model and control approach for SSSC to contribute effectively in AGC of a deregulated power system," *International Journal of Electrical Power & Energy Systems*, vol. 95, pp. 239-253, 2018.

[32] I. Pan, S. Das, "Fractional-order load-frequency control of interconnected power systems using chaotic multi-objective optimization," *Applied Soft Computing*, vol. 29, pp. 328-344, 2015.

[33] L. Chaib, A. Choucha, S. Arif, "Optimal design and tuning of novel fractional order PID power system stabilizer using a new metaheuristic bat algorithm," *Ain Shams Engineering Journal*, vol. 8, no. 2, pp. 113-125, 2017.

[34] J. Morsali, K. Zare, MT. Hagh, "Applying fractional order PID to design TCSC-based damping controller in coordination with automatic generation control of interconnected multi-source power system," *Engineering Science and Technology, an International Journal*, vol. 20, no. 1, pp. 1-17, 2017.

[35] M. Saadatmand, B. Mozafari, G. B. Gharehpetian, S. Soleymani, "Optimal fractional-order PID controller of inverter-based power plants for power systems LFO damping," *Turkish Journal of Electrical Engineering & Computer Sciences*, vol. 28, no. 1, pp. 485-499, 2020.

[36] M. Saadatmand, B. Mozafari, G. B. Gharehpetian, S. Soleymani, "Optimal Coordinated Tuning of Power System Stabilizers and Wide-area Measurement-based Fractional-order PID Controller of Large-scale PV Farms for LFO Damping in Smart Grids," *International Transactions on Electrical Energy Systems*, vol.31, no. 2, e12612, 2021.

[37] Accommodating High Levels of Variable generation, North American Electric Reliability Corporation (NERC), Special Report, Princeton, NJ, USA, 2008.

[38] P. Pourbeik, et al., "Generic dynamic models for modeling wind power plants and other renewable technologies in large-scale power system studies," *IEEE Trans. Energy Convers.*, vol. 32, no. 3, pp. 1108-1116, 2017.

[39] P. Pourbeik, "Model user guide for generic renewable energy system models", Electr. Power Res. Inst., Palo Alto, CA, USA, Tech. Rep. 3002006525, 2015.

[40] Y.T. Tan, D. Kirschen, N. Jenkins, "A model for PV generation suitable for stability analysis," *IEEE Transactions on Energy Conversion*, vol. 19, no.4, pp.748-755, 2004.

[41] K. Clark, N. W. Miller, R. Walling, "Modeling of GE solar photovoltaic plants for grid studies", General Electric International. Inc, Schenectady, NY, USA, 2010.

[42] K. Clark, R. A. Walling, N. W. Miller, "Solar photovoltaic (PV) plant models in PSLF", in *2011 IEEE Power and Energy Society General Meeting*, Detroit, MI, USA, pp. 1-5, 2011.

[43] WECC Renewable Energy Modeling Task Force. "Generic Solar Photovoltaic System Dynamic Simulation Model Specification*", Salt Lake City: Western Electricity Coordinating Council*; 2012.

[44] K. S. Miller, B. Ross, "*An Introduction to the fractional calculus and fractional differential equations*", New York, USA: John Wiley, 1993.

[45] C. Canizares, et al., "Benchmark Models for the Analysis and Control of Small-Signal Oscillatory Dynamics in Power Systems," *IEEE Transactions on Power Systems*, vol. 32, no. 1, pp. 715-722, 2017.

[46] P. Kundur, "*Power system stability and control*", New York: McGraw-Hill, 1994.

[47] S. K. Kerahroudi, M. M. Alamuti, F. Li, G. A. Taylor, M. E. Bradley, "Application and Requirement of DIgSILENT PowerFactory to MATLAB/Simulink Interface," In: F. M. Gonzalez-Longatt, J. L. Rueda (editors), PowerFactory Applications for Power System Analysis. Cham, Switzerland: Springer, pp. 297-322, 2014.

[48] D. Cai, "*Wide area monitoring, protection and control in the future Great Britain power system*," Ph.D., University of Manchester, Manchester, UK, 2012.

[49] H. K. Abdulkhader, J. Jacob, A. T. Mathew, "Fractional-order lead-lag compensator-based multi-band power system stabilizer design using a hybrid dynamic GA-PSO algorithm," *IET Gener., Transmiss. Distrib.*, vol. 12, no. 13, pp. 3248-3260, 2018.

[50] Y. Nie, Y. Zhang, Y. Zhao, B. Fang, L. Zhang, "Wide-area optimal damping control for power systems based on the ITAE criterion," *International Journal of Electrical Power & Energy Systems*, vol. 106, pp. 192-200, 2019.

[51] G. Rogers, "*Power system oscillations*", Boston: Kluwer Academic Publishers, 2000.

[52] T. K. Das, G. K. Venayagamoorthy, U. O. Aliyu, "Bio-inspired algorithms for the design of multiple optimal power system

stabilizers: SPPSO and BFA," *IEEE Transactions on Industry Applications*, vol. 44, no. 5, pp. 1445-1457, 2008.

[53] P. Sarzaeim, O. Bozorg-Haddad, X. Chu, "Teaching-learning-based optimization (TLBO) algorithm", In *Advanced optimization by nature-inspired algorithms*, pp. 51-58, Springer, Singapore, 2018.

[54] R. Rao, "Review of applications of TLBO algorithm and a tutorial for beginners to solve the unconstrained and constrained optimization problems", *Decision science letters*, vol. 5, no. 1, pp. 1-30, 2016.

[55] H. Shayeghi, H. A. Shayanfar, A. Safari, R. Aghmasheh, "A robust PSSs design using PSO in a multi-machine environment", *Energy Conversion and Management*, vol. 51, pp. 696-702, 2010.

[56] P. Wang, D. P. Kwok, "Optimal design of PID process controllers based on genetic algorithm," *Control Engineering Practice*, vol. 2, no. 4, pp 641-648, 1994.

[57] Y. Hashmy, Z. Yu, D. Shi, Y. Weng, "Wide-area measurement system-based low frequency oscillation damping control through reinforcement learning", *IEEE Transactions on Smart Grid*. vol. 11, no. 6, pp. 5072-5083, 2020.

[58] M. Raeispour, H. Atrianfar, H. R. Baghaee, G. B. Gharehpetian, "Resilient H∞ Consensus-based Control of Autonomous AC Microgrids with Uncertain Time-Delayed Communications", *IEEE Transactions on Smart Grid,* vol. 11, no. 5, pp. 3871-3884, 2020.

MAHDI SAADATMAND received the M.Sc. degree in electrical engineering from Amirkabir University of Technology, Tehran, Iran in 2013 and the Ph.D. degree in electrical engineering from Science and Research Branch, Islamic Azad University, Tehran, Iran in 2020. He has authored more than 16 scientific journal and conference papers. His research interests include Power System Dynamics, Smart Grids, Renewable Energy Technologies and Fractional-order control. Since 2019, he has been serving as a reviewer for several high-quality journals.

GEVORK B. GHAREHPETIAN (Senior Member, IEEE) received his BS, MS and PhD degrees in electrical engineering in 1987, 1989 and 1996 from Tabriz University, Tabriz, Iran and Amirkabir University of Technology (AUT), Tehran, Iran and Tehran University, Tehran, Iran, respectively, graduating all with First Class Honors. As a PhD student, he has received scholarship from DAAD (German Academic Exchange Service) from 1993 to 1996 and he was with High Voltage Institute of RWTH Aachen, Aachen, Germany. He has been holding the Assistant Professor position at AUT from 1997 to 2003, the position of Associate Professor from 2004 to 2007 and has been Professor since 2007.

He was selected by the MSRT (Ministry of Science Research and Technology) as the distinguished professor of Iran, by IAEEE (Iranian Association of Electrical and Electronics Engineers) as the distinguished researcher of Iran, by Iran Energy Association (IEA) as the best researcher of Iran in the field of energy, by the MSRT as the distinguished researcher of Iran, by the Academy of Science of the Islamic Republic of Iran as the distinguished professor of electrical engineering, by National Elites Foundation as the laureates of Alameh Tabatabaei Award and was awarded the National Prize in 2008, 2010, 2018, 2018, 2019 and 2019, respectively. Based on the Web of Science database (2005-2019), he is among world's top 1% elite scientists according to ESI (Essential Science Indicators) ranking system.

Prof. Gharehpetian is distinguished, senior and distinguished member of CIGRE, IEEE and IAEEE, respectively. Since 2004, he has been the Editor-in-Chief of the Journal of IAEEE. He is the author of more than 1200 journal and conference papers. His teaching and research interests include Smart Grid, Microgrids, FACTS and HVDC Systems, Monitoring of Power Transformers and its Transients.

PIERLUIGI SIANO (M'09-SM'14) received the M.Sc. degree in electronic engineering and the Ph.D. degree in information and electrical engineering from the University of Salerno, Salerno, Italy, in 2001 and 2006, respectively. He is a Professor and Scientific Director of the Smart Grids and Smart Cities Laboratory with the Department of Management & Innovation Systems, University of Salerno. His research activities are centered on demand response, on energy management, on the integration of distributed energy resources in smart grids, on electricity markets and on planning and management of power systems. In these research fields he has co-authored more than 500 articles including more than 300 international journal papers that received in Scopus more than 9450 citations with an H-index equal to 47. He received the award as 2019 Highly cited Researcher by ISI Web of Science Group. He has been the Chair of the IES TC on Smart Grids. He is Editor for the Power & Energy Society Section of IEEE Access, IEEE TRANSACTIONS ON INDUSTRIAL INFORMATICS, IEEE TRANSACTIONS ON INDUSTRIAL ELECTRONICS, Open Journal of the IEEE IES and of IET Renewable Power Generation.

HASSAN HAES ALHELOU (Senior Member, IEEE) is a faculty member at Tisheen University, Lattakia, Syria. He is included in the 2018 and 2019 Publons list of the top 1% best reviewer and researchers in the field of engineering. He was the recipient of the Outstanding Reviewer Award from Energy Conversion and Management Journal in 2016, ISA Transactions Journal in 2018, Applied Energy Journal in 2019, and many other Awards. He was the recipient of the best young researcher in the Arab Student Forum Creative among 61 researchers from 16 countries at Alexandria University, Egypt, 2011. He has published more than 100 research papers in the high quality peer-reviewed journals and international conferences. He has also performed reviews for high prestigious journals including IEEE Transactions on Industrial Informatics, IEEE Transactions on Industrial Electronics, Energy Conversion and Management, Applied Energy, International Journal of Electrical Power & Energy Systems. He has participated in more than 15 industrial projects. His major research interests are Power systems, Power system dynamics, Power system operation and control, Dynamic state estimation, Frequency control, Smart grids, Micro-grids, Demand response, Load shedding, and Power system protection.